International Journal of Materials Science and Applications
2014; 3(2): 14-19
Published online January 30, 2014 (http://www.sciencepublishinggroup.com/j/ijmsa)
doi: 10.11648/j.ijmsa.20140302.11

Effects of carrier gas flow-rate and oxygen admixture ratio on particle properties in Ar-O_2 plasma

M. Rafiqul Alam[1], Feroza Begum[2], Quazi Delwar Hossain[1], M. Mofazzal Hossain[2, *]

[1]Department of Electrical and Electronic Engineering, Chittagong University of Engineering and Technology Chittagong, Bangladesh
[2]Department of Electronics and Communications Engineering, East West University, Aftabnagar, Dhaka-1212, Bangladesh

Email address:
dmmh@ewubd.edu (M. M. Hossain)

To cite this article:
M. Rafiqul Alam, Feroza Begum, Quazi Delwar Hossain, M. Mofazzal Hossain. Effects of Carrier Gas Flow-Rate and Oxygen Admixture Ratio on Particle Properties in Ar-O_2 Plasma. *International Journal of Materials Science and "pplications*. Vol. 3, No. 2, 2014, pp. 14-19. doi: 10.11648/j.ijmsa.20140302.11

Abstract: Taking into account the strong plasma-particle interactions and particle loading effects, a plasma-particle interactive flow model for argon-oxygen plasma has been developed. We can predict the particle temperature, velocity, trajectory and plasma temperature isotherm by solving the model numerically during the in-flight thermal treatment of granulated micro-particles under local thermal equilibrium (LTE) conditions. It is found that the carrier gas flow-rate strongly affects the particle temperature, the admixture ratio of argon to oxygen and the plasma temperature isotherm.

Keywords: Particle Temperature, Particle Trajectory, Admixture Ratio, Carrier Gas Flow Rate

1. Introduction

The application trends of thermal plasma for research and industrial purposes are pronouncing [1]. Especially as a clean reactive heat source [2], induction thermal plasma (ITP) has been extensively using for the synthesis and thermal treatment of micro-particles. Materials with improved physical and mechanical properties have a growing demand for high tech industries as electronics, transportation, glass and radio communications. Induction thermal plasma technology ensures essentially the in-flight one-step melting, short melting time, and less pollution compared with the traditional technologies. The thermal treatment of injected particles mainly depends on the plasma-particle heat transfer efficiency. On the other hand, it is depend on the particles trajectory, plasma temperature and diameter of the injected particles. Therefore numerical modeling for the prediction of the trajectory and temperature history of the particles injected into the ITP torch is very crucial. Yoshida *et al* [3] developed a model of particle heating in induction plasmas and described the particle trajectory along the centerline of the torch only. Proulx *et al* [4] discussed the particle loading effects in argon induction plasma. Boulos [5] developed a model and predicted the trajectory and temperature history of injected particles for argon plasma. Moreover, Hossain *et al* [6] is developed a plasma-particle interactive flow model where any kind of gases can be used. In this paper, we will investigate the effects of carrier gas and oxygen to argon admixture ratio on particle parameters in argon-oxygen plasma.

2. Modeling

A schematic illustration of ITP torch is shown in Fig. 1. The dimensions of the torch and the discharge conditions are listed in Table-1. The following assumptions are made here for equilibrium thermal plasma with the axial injection of argon and oxygen mixture at atmospheric pressure.

The model solves the conservation equations and vector potential in the form of Maxwell's equations simultaneously under the LTE conditions, including a metal nozzle inserted into the torch. It is assumed that the plasma flow is 2-dimensional, axi-symmetric, laminar, steady, optically thin, and 2-dimensional electromagnetic (EM) fields.

2.1. Plasma Model

The fields of flow, temperature, and concentration in the induction thermal plasma are calculated by solving the two-dimensional continuity, momentum, species and energy conservation equations coupled with the Maxwell's equations.

Mass conservation:

$$\nabla \cdot \rho u = S_p^C \tag{1}$$

Energy conservation:

$$\rho \mathrm{u} \cdot \nabla h = \nabla \cdot \left(\frac{\kappa}{C_p} \nabla h \right) + \mathrm{J} \cdot \mathrm{E} - Q_r - S_p^E \tag{2}$$

Momentum conservation:

$$\rho \mathrm{u} \cdot \nabla \mathrm{u} = -\nabla p + \nabla \cdot \mu \nabla \mathrm{u} + \mathrm{J} \times \mathrm{B} + S_p^M \tag{3}$$

Species Conservation:

$$\rho \mathrm{u} \cdot \nabla y = \nabla \cdot \left(\rho D_m \nabla y \right) + S_p^C \tag{4}$$

Maxwell's EM Field equations [7]:

$$\nabla^2 \, ''_c = i \mu_0 \sigma \omega ''_c \tag{5}$$

where, ∇: vector operator, u: velocity vector, ρ: mass density, μ: viscosity, σ: electrical conductivity, κ: thermal conductivity, h: enthalpy, p: pressure, C_p: specific heat at constant pressure, D_m: multi component diffusion coefficient, y: mass fraction, J: current density vector, E: electric field vector, B: magnetic field vector, Q_r: volumetric radiation loss, $''_c$: complex amplitude of vector potential, μ_0: permeability of free space, ω: $2\pi f$ (f: frequency), i: complex vector ($\sqrt{-1}$). The particle source terms S_P^C, S_P^M, and S_P^E are the contributions of particles to the mass and species, momentum and energy conservation equations respectively.

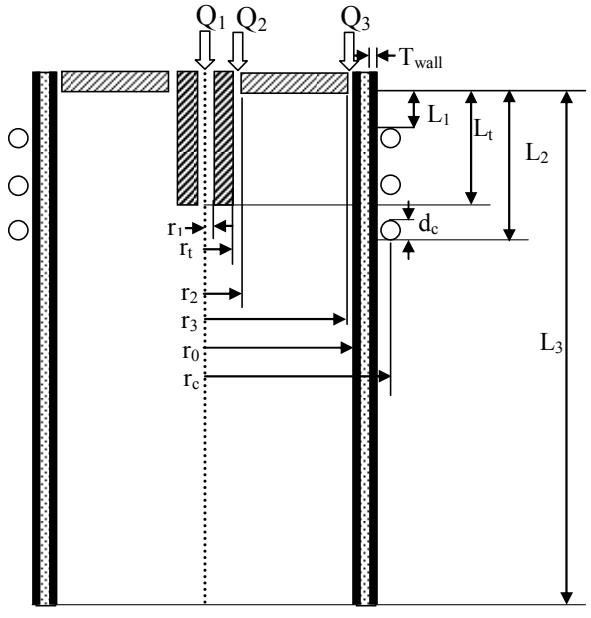

Fig 1. *Schematic geometry and dimensions of ITP torch.*

2.2. Particle Model

The following assumptions are made in the analysis of plasma-particle interactions in the ITP torch. The particle motion is two-dimensional, only the viscous drag force and gravity affect the motion of an injected particle. In this case, the temperature gradient inside the particle is neglected, and the particle charging effect caused by the impacts of electrons or positive ions is also negligible. Electromagnetic drag forces caused by the injected charging particle are negligible compared with those by neutrals. Therefore momentum equations for a single spherical particle injected vertically downward into the plasma torch can be expressed as follows:

$$\frac{dv_p}{dt} = -\frac{3}{4} C_D (v_p - v) U_R \left(\frac{\rho}{\rho_p d_p} \right) \tag{6}$$

$$\frac{du_p}{dt} = -\frac{3}{4} C_D (u_p - u) U_R \left(\frac{\rho}{\rho_p d_p} \right) + g \tag{7}$$

$$U_R = \sqrt{(u_p - u)^2 + (v_p - v)^2} \tag{8}$$

The net energy transferred to particles can be expressed as follows:

$$Q = \left\{ \pi d_p^2 h_c \left(T - T_p \right) \right\} - \left\{ \pi d_p^2 \sigma_s \varepsilon \left(T_p^4 - T_a^4 \right) \right\} \tag{9}$$

The particle temperature and diameter are predicted according to the following energy balances:

$$\frac{dT_p}{dt} = \frac{6Q}{\pi \rho_p {d_p}^3 C_{pp}} \quad \text{for Tp<1000} \tag{10}$$

$$\frac{dT_p}{dt} = \frac{6Q}{\pi \rho_p {d_p}^3 C'_{pp}} \quad \text{for } 1000 \le \mathrm{Tp} \le 1600 \tag{11}$$

$$\frac{dT_p}{dt} = \frac{6Q}{\pi \rho_p {d_p}^3 C''_{pp}} \quad \text{for } 1600 \le \mathrm{Tp} \le \mathrm{Tb} \tag{12}$$

$$\frac{dd_p}{dt} = -\frac{2Q}{\pi \rho_p {d_p}^2 H_v} \quad \text{for Tp = Tb} \tag{13}$$

where u_p: axial velocity component of particle, v_p: radial velocity component of particle, g: acceleration of gravity, ρ_p: particle mass density, d_p: particle diameter, C_D: Drag coefficient, Q: net heat exchange between the particle and its surroundings, T_p: particle temperature, T_b: boiling point temperature, T: plasma temperature, T_a: ambient temperature, ε: particle porosity; σ_s: Stefan–Boltzmann constant, C_{pp}: particles solid specific heat, C'_{pp}: particles effective heat of vitrification, C''_{pp},: particles liquid specific heat, and H_v: latent heat of vaporization.

The convective heat transfer coefficient is predicted as follows:

$$h_c = \frac{\kappa_f}{d_p} Nu_f f_3 \tag{14}$$

Where Nu_f and f_3 are the Nusselt correlation and non-continuum effect respectively [8].

2.3. Particle Source Terms

For loading effects, the particles source terms for the mass, momentum, energy and species conservation equations have been calculated by using particle source in cell approach [9] where the particles are considered as a source of mass, momentum and energy.

Let us assume N_t^0 is the total number of particles injected per unit time, n_d is the particle size distribution, and n_r is the fraction of N_t^0 injected at each point through the injection nozzle. Thus, the total number of particles per unit time travelling along the trajectory (l, k) corresponding to a particle diameter d_l injected at the inlet point r_k is:

$$N^{(l,k)} = n_{d_l} n_{r_k} N_t^0 \tag{15}$$

For the sake of computation, the particle concentration n_r in the inlet is assumed to be uniform and to be separated into five injection points, which are at radial positions of 0.3, 0.45, 0.6, 0.75 and 0.9 mm. In the present computation, the particles diameter distribution is assumed to be Maxwellian. The powder is assumed to be composed of seven different size particles according to its diameter and deviation. The average particle diameter is 58 μm and the maximum deviation is 67%. As a result, there are 35 different possible trajectories of the injected particles. Thus the injection velocity of the particles is assumed to be equal to the injection velocity of carrier gas.

2.4. Thermodynamics and Transport Properties

Thermodynamic and transport properties of argon and oxygen gases are required for the simulation of mass density, specific heat at constant pressure, viscosity, electrical-thermal conductivity and radiative loss coefficient. The temperature dependence transport properties are calculated under LTE conditions by using Chapman-Enskog first approximation to Boltzmann equation [10].

2.5. Physical Properties of Powder

The physical properties of soda–lime–silica glass powders are - mass density: 2300 kg/m^3, specific heat: 800 J/kg-K, porosity: 80%, fusion temperature: 1000–1600 K, boiling temperature: 2500 K, and heat of vaporization: 1.248×10^7 J/kg. Particle porosity has been measured by applying Pycnometer method. All the properties of soda–lime–silica glass powders have been measured by Asahi Glass Company (Japan).

2.6. Boundary Conditions

The boundary conditions for the mass, momentum, energy and species conservation equations are: at the inlet-gas temperature is set to 300 K and uniform velocity profiles are assumed based on the given flow rates; on the axis of symmetry- the symmetry conditions are imposed; on the walls- no-slip condition is assumed; the outer wall temperature is set to 350 K; and at the exit- axial gradients of all fields are set equal to zero. The inserted nozzle is assumed to be water cooled at 300 K. On the nozzle wall, the velocity is set to zero. The boundary conditions for the vector potential form of Maxwell's equation are the same as those described in reference [11].

2.7. Computational Methodology

The governing conservation equations are solved by using the semi-implicit method for pressure linked equation revised (SIMPLER) algorithm [12]. The governing equations and the electric field intensity equation associated with boundary conditions are discretized into a finite difference form using the control-volume technology. Non-uniform grid points 44/ 93 are used for radial and axial directions, respectively. Grids are made finer close to the centre and the coil region.

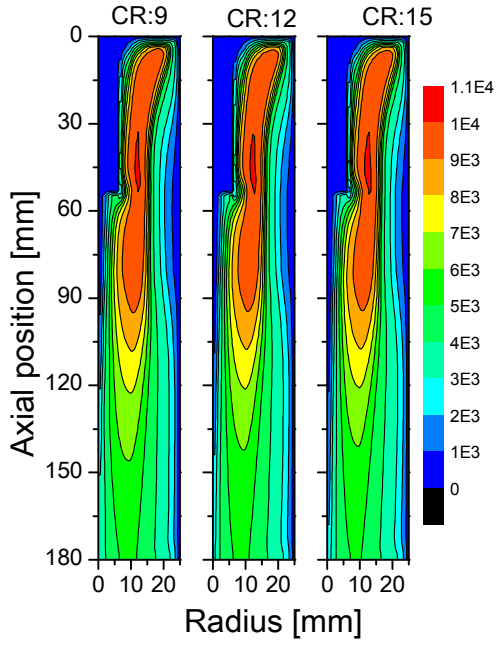

Fig 2. *Effects of carrier gas flow-rate on plasma temperature isotherms.*

3. Simulated Results and Discussion

Fig. 2 shows the effects of carrier gas flow-rate (CR) on the plasma temperature isotherms for carrier gas flow-rate of 9, 12 and 15 lpm (litter per minute). It is found that with the increasing of carrier gas flow-rate, the high temperature plasma zone become smaller. This happens due to the excess energy required to ionize the additional gas injected into the torch with a constant supplied energy (10 kW). Fig. 3 shows the effects of oxygen to argon admixture ratio on the plasma temperature isotherms for a carrier gas flow-rate of 9 lpm. In case of oxygen, it first dissociates and then ionizes, thus it requires more energy for dissociation process which is not required in argon. Therefore plasma

temperature reduces with the increase of oxygen to argon admixture ratio. Fig. 4 illustrates the effects of carrier gas flow-rate on the particle trajectory. It is observed that with the increasing of flow-rate particle trajectories remain close to the centerline of the torch. This is because larger axial drug force at higher carrier gas flow-rate forces the particles to go down. Fig. 5 shows that at certain carrier gas flow-rate, the trajectories of smaller particles become wider than those of the large particles. This also happens due to the smaller momentum of smaller particles in the downward direction. Fig. 6 presents the effects of carrier gas flow-rate on the particle temperature. It is found that the downward in-flight particle temperature become lower at higher carrier gas flow-rate. At higher carrier gas flow-rate, plasma temperature decreases as a result, heat transfer to particles also decreases, which yields lower particle temperature. Fig. 7 reveals the effects of particle size on the particle temperature. It is noticed that the smaller particles attain the boiling point temperature whether the larger particles do not. This is due the large heat capacity of larger particles. Thus it emphasizes that the treatment of smaller particles is much easier than the larger particles. Fig. 8 shows effects of oxygen admixture ratio on the plasma temperature profile within the torch for oxygen flow-rate of 2, 3 and 4 lpm. It is found that the increase of oxygen admixture ratio in the plasma torch causes the plasma temperature to decrease, especially in the down stream of the plasma torch. This happens due the higher specific heat of oxygen. Fig. 9 shows the effects of carrier gas flow-rate on the axial plasma velocity. It is seen that the axial plasma velocity decreases with the increase of carrier gas flow-rate in the down stream of the torch. It happens due the higher momentum attributed at the higher carrier gas flow-rate.

Table 1. *Torch dimensions and discharge conditions*

Distance to initial coil position (L_1)	19 mm
Length of injection tube (L_t)	52 mm
Distance to end of coil position (L_2)	65 mm
Torch length (L_3)	190 mm
Coil diameter (d_c)	5 mm
Wall thickness of quartz tube (T_{wall})	1.5 mm
Inner radius of injection tube (r_1)	1 mm
Outer radius of injection tube (r_t)	4.5 mm
Outer radius of inner slot (r_2)	6.5 mm
Inner radius of outer slot (r_3)	21.5 mm
Torch radius (r_0)	22.5 mm
Coil radius (r_c)	32 mm
Plasma power	10 kW
Working frequency	4 MHz
Working pressure	0.1 MPa
Flow rate of carrier gas (Q_1)	6 ~ 15 lpm of Argon
Flow rate of plasma gas (Q_2)	2 lpm of Argon
Flow rate of sheath gas (Q_3)	22 lpm Argon & 2~4 lpm Oxygen

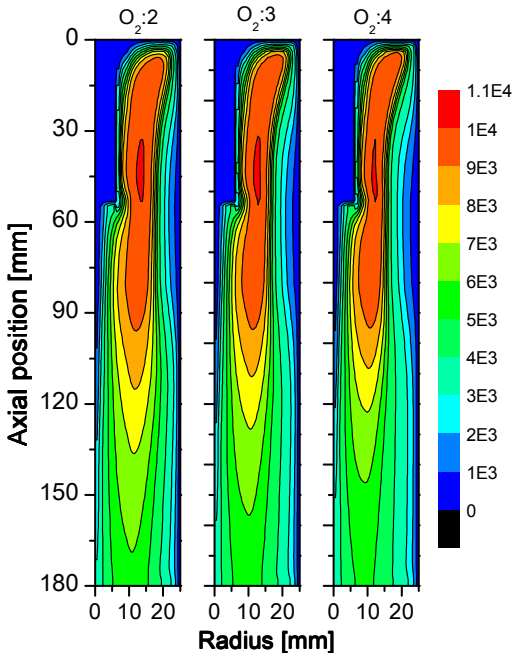

Fig 3. *Effects of oxygen admixture ratio on plasma temperature isotherms for carrier gas 9 lpm.*

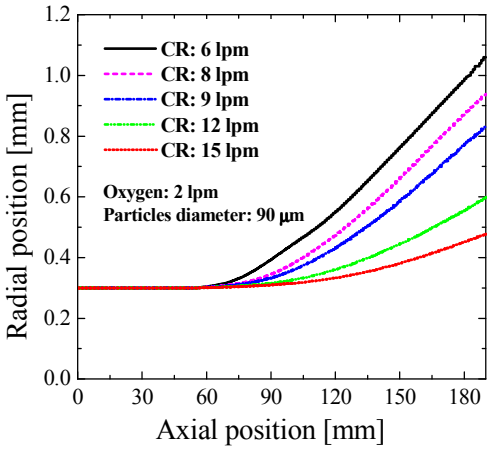

Fig 4. *Effects of carrier gas flow-rate on particle trajectories.*

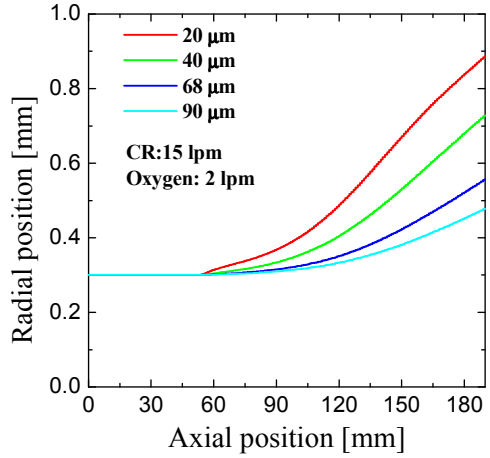

Fig 5. *Effects of carrier gas on particle trajectory for different diameter of particles.*

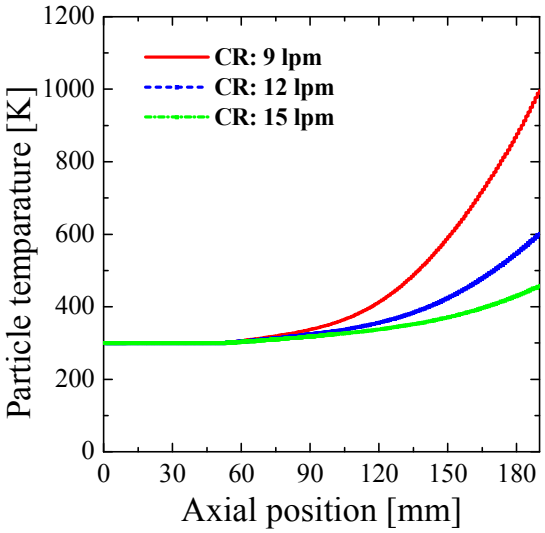

Fig 6. *Effects of carrier gas on the particle temperature.*

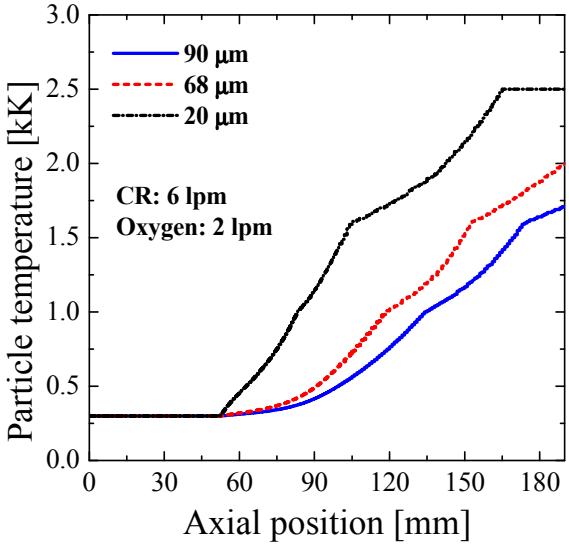

Fig 7. *Effects of particle size on particle temperature.*

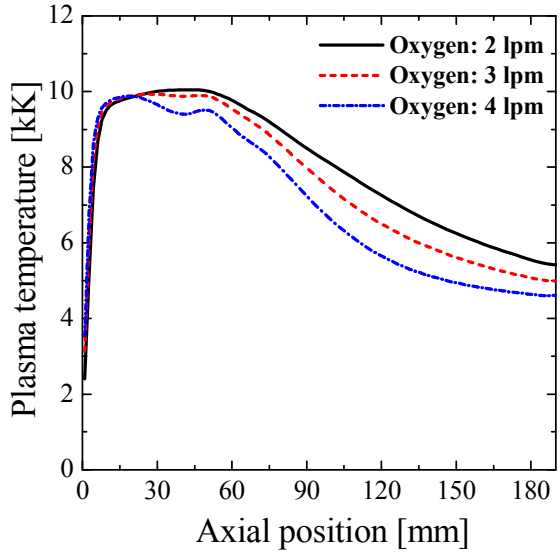

Fig 8. *Effects of oxygen admixture ratio on plasma temperature.*

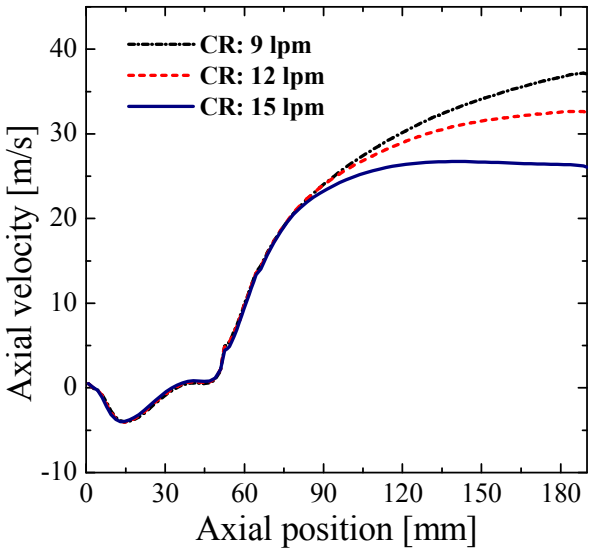

Fig 9. *Effects of carrier gas flow-rate on axial velocity.*

4. Conclusion

A plasma-particle interactive flow model has been developed to simulate the particle trajectories, particle temperature histories, optimize the carrier gas flow-rate and oxygen to argon admixture ratio. To make the process of thermal treatment efficient by argon-oxygen induction thermal plasma, this model could be used as an important tool. Numerically, it was found that the heat transfer to particles was decreased at increased carrier gas flow-rate and higher admixture ratio of oxygen.

References

[1] K. C. Paul, T. Takashima and T. Satkuta, "Copper vapor effect on RF inductively coupled SF_6 plasma," *IEEE Trans Plasma Sci*., vol.26, pp.1000-1009, 1998.

[2] T. Watanzabe and K. Fujiwara, " Nucleation and growth of oxide nanoparticles prepared by induction thermal plasma," *Chem. Eng. Comm.*, vol. 191, pp. 1343-1361, 2004

[3] T. Yoshida and K. Akashi, "Particle heating in a radio-frequency plasma torch," *J. Appl. Phys.* vol. 48, 3352, 1997.

[4] P. Proulx, J. Mostaghimi and M. I Boulos, "Plasma-particle interaction effects in induction plasma modeling under dense loading conditions," *Int. J. Heat Mass Transfer* vol. 28, 1327,1985.

[5] M. I. Boulos, "Heating of powders in the fire ball of induction plasma," *IEEE Trans. on Plasma Sci,* PS -6 pp 93, 1978.

[6] M. M. Hossain, Y. Yao, M. R Alam, M. M. Alam and Y. Watanabe, "Modeling and numerical analysis of thermal treatment and granulated porous particles by induction plasma," *5th International conference on Electrical and Computer Engineering, ICECE* 20-22, December 2008 Dhaka, Bangladesh.

[7] J. Mostaghimi, K. C. Paul and T. Sakuta, "Transient response of radio frequency inductively coupled plasma to a sudden change in power." *J. Appl. Phys.*, vol 83, pp 1898-1908, 1998.

[8] M. M. Hossain, Y. Yao, T. Watanabe, "A numerical analysis of plasma-particle heat exchange during in-flight treatment of granulated powders by argon-oxygen induction thermal plasmas*," Thin Solid Films,* vol 516, pp 6634–6639, 2008.

[9] C. T. Crowe, M. P. Sharma, D. E. Stock, "The particle source-In cell (PSI CELL) model for gas-droplet flows," *J. Fluids Eng*. vol. 99, pp. 325-323, 1977.

[10] Y. Tanaka, K. C Paul and T. Sakuta, "Thermodynamic and transport properties of N_2/O_2 mixtures at different admixture ratio," *Trans. IEE Japan,* 120-B, pp. 24-30, 2000.

[11] M. M. Hossain, Y. Yao, T. Watanabe, F. Funabiki and T. Yano, "In-flight melting mechanism of soda-lime-silica glass powders for glass production by argon-oxygen induction thermal plasmas," *Chemical Engineering Journal*, vol. 150, Issue 2-3, pp. 561-568, 2009.

[12] S. V. Patankar, *Numerical fluid flow and heat transfer*, Hemisphere, New York, 1980.